The International Journal of Advanced Manufacturing Technology (2018) 99:313–326
https://doi.org/10.1007/s00170-018-2494-8

ORIGINAL ARTICLE

Machining of GTAW additively manufactured Ti-6Al-4V structures

N. Hoye[1,2] · D. Cuiuri[1,2] · R. A. Rahman Rashid[3,2] · S. Palanisamy[3,2]

Received: 10 May 2018 / Accepted: 18 July 2018 / Published online: 2 August 2018

Abstract
Titanium components such as spars, brackets and landing gear assemblies, containing deep pockets, thin walls and fixturing holes are used in almost all aircraft. The traditional method of fabricating these parts involves significant amount of machining resulting in unsustainably high buy-to-fly ratios. For this reason, additive manufacturing (AM) processes are being considered for making near-net shape components. Gas tungsten arc welding (GTAW) is an economical AM process with higher deposition rates which has been employed to fabricate these titanium components. However, the GTAW-fabricated parts require post-finish machining to meet the strict dimensional tolerances as per design. On the other hand, it is well known that titanium is a difficult-to-machine material. Therefore, the primary objective of this study was to evaluate the machinability of Ti-6Al-4V thin wall and pad structures produced using GTAW additive manufacturing in terms of cutting forces, surface roughness and tool wear during milling and drilling operations. The cutting forces were found to be lower by about 13–21% during milling owing to the lower hardness of the additively manufactured wall in comparison to the wrought T-fillet structure. In contrast, the normal drilling force was higher by about 10–15% for the additively manufactured pad due to its higher hardness as compared to the wrought Ti-6Al-4V billet, though the tool wear was noticed to be higher when drilling the wrought billet. Nevertheless, it was concluded that the machinability of the GTAW-fabricated Ti-6Al-4V was better than the wrought counterpart.

Keywords Gas tungsten arc welding · Additive manufacturing · Ti-6Al-4V · Milling · Drilling

1 Introduction

Titanium alloys possess a wide range of desirable mechanical and physical properties including high strength-to-weight ratios, moderate ductility, good fatigue and fracture resistance and excellent corrosion resistance in a wide range of environments. Due to this fact, titanium alloys are used in various industries, primarily aerospace, military, power generation, chemical/petrochemical processing and biomedicine [1]. Of these, aerospace is the largest user, accounting for almost 60% of metallic titanium consumption by mass [2, 3]. However, the fabrication of titanium aircraft components has unsustainably high buy-to-fly ratios with typically more than 80% of titanium being removed by machining [4, 5]. This has resulted in significantly high secondary processing costs for titanium aerospace components [6]. With the increased demand for components made from titanium and its alloys, significant efforts are being made to reduce the costs associated with these materials by development of alternate cost-effective manufacturing techniques. One area of particular interest is the use of near net shape forming and additive manufacturing techniques which have seen a rapid emergence in recent years [7, 8]. Using these, three dimensional freeform structures can be produced by deposition and bonding of successive layers of material, giving increased material utilisation and enhanced design flexibility.

Various additive manufacturing (AM) techniques have been proposed for the fabrication of near-net shape titanium parts including direct laser deposition [9], selective laser melting [10], arc-wire AM [11] and electron beam melting [12]. These processes can be classified by the heat source (laser, electron beam, or arc-welding), feedstock type (powder or wire) and the deposition technique. AM equipment incorporating either laser or electron beam heat sources are expensive,

✉ S. Palanisamy
spalanisamy@swin.edu.au

[1] Faculty of Engineering, University of Wollongong, Wollongong, New South Wales, Australia

[2] Defence Materials Technology Centre, Hawthorn, Victoria 3122, Australia

[3] School of Engineering, Faculty of Science, Engineering and Technology, Swinburne University of Technology, Hawthorn, Victoria 3122, Australia

Table 1 Chemical composition of Ti-6Al-4V filler wire

Alloy	Ti	C	Fe	H	N	O	Al	V
Ti-6Al-4V	89.2	0.1	0.3	0.015	0.03	0.25	6.1	4.0

rendering them undesirable for most commercial applications. Furthermore, wire-feed processes are more economical and less susceptible to atmospheric contamination when compared with powder-based processes [13]. Therefore, the arc-wire based methods are considered to be most suited for the manufacture of structural components from titanium alloys due to their increased flexibility through robotic and out-of-chamber operation, high deposition rates and low capital costs [14, 15].

Gas tungsten arc welding (GTAW) is one such arc-wire AM process which utilises a non-consumable tungsten electrode and an externally fed wire filler metal to deposit uniform weld tracks under an inert gas shielding. Moreover, the ability to independently control the heat input and deposition rate in GTAW presents a significant advantage over other arc-wire AM processes such as gas metal arc welding (GMAW), controlled dip transfer/cold metal transfer (CMT), and plasma arc metal deposition (PAM) [16]. Ti-6Al-4V exhibits good weldability, especially by additive manufacturing techniques such as GTAW and selective laser melting, due to its low hardenability and the ductile nature of its α' martensite phase, which is significantly lower than that of the $\alpha + \beta$ microstructure [17–19]. Additionally, this alloy captures more than 50% of the global titanium market [20]. Therefore, Ti-6Al-4V is an ideal candidate alloy for the investigation of arc-wire based additive manufacture of structural titanium components.

In a recent study, Williams et al. [21] have reported fabricating several Ti-6Al-4V aircraft parts such as wing spars and landing gear assemblies using GTAW AM process. Such large thin-walled features are ideally suited to production through GTAW-wire based additive manufacture where significant savings in material and machining can be achieved. Although GTAW has been effectively used to additively manufacture these titanium parts, the GTAW-build components had poor surface quality and required post-finish machining to achieve the designed surface and dimensional tolerances. On the other hand, it is well known that titanium is a difficult-to-machine material due to its low thermal conductivity and high chemical reactivity with most cutting tools [22–24]. These properties are often seen to contribute to reduced tool life and poor surface finish. Bolar et al. [25] reported that finish machining of thin-walled structures is very complicated wherein the free end of the wall is subjected to the chattering effect as well as the intermittent cutting teeth engagement with the workpiece adversely affects the quality of the machined surface. Moreover, Wojciechowski et al. [26] reported that implementation of appropriate machining parameters for a particular material can yield significant improvement in process efficiency. Since machinability is inextricably linked to material properties, it is apparent that the machining response of Ti-6Al-4V produced by GTAW AM may differ from that of conventional wrought material and must be characterised.

In summary, with the advent of additive manufacturing processes to fabricate near-net shaped titanium components, there is a strong need to understand the machining behaviour of such difficult-to-machine materials when subjected to finish machining operations. Therefore, the primary objective of this study is to investigate aspects of machinability of additively manufactured Ti-6Al-4V parts produced using the established GTAW arc-wire process and compare to those resulting from wrought workpieces fabricated using conventional processes. As the AM fabricated titanium parts will most likely be aircraft components such as spars, strut components, brackets and monolithic assemblies that contain deep pockets, thin walls, and holes, milling and drilling are the machining operations that will be carried out on these GTAW-fabricated titanium parts. The cutting forces generated during these machining

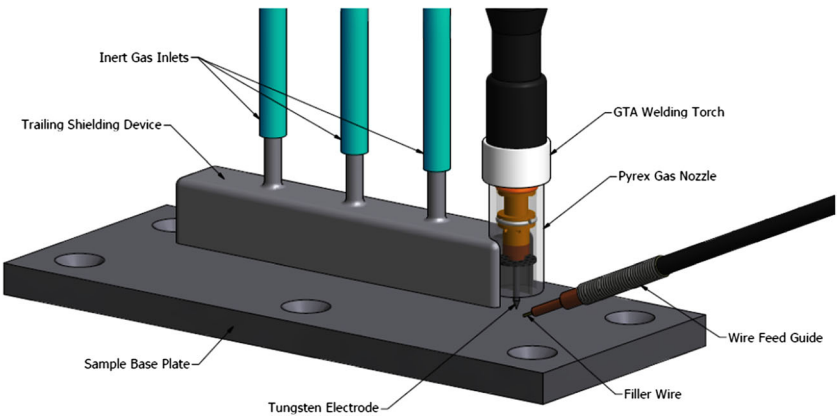

Fig. 1 General arrangement of the welding torch, wire feed and inert trailing shielding used to produce additively manufactured samples

Table 2 Summary of GTAW process parameters

Polarity	DCEN
Electrode	2% Ceriated, 2.4 mm Ø
Shielding gas	Welding Grade Argon
Flow rate—torch nozzle	8 L/min
Flow rate—trailing shield front	10 L/min
Flow rate—trailing shield rear	7 L/min
Pre-flow duration	3 s
Up slope duration	2 s
Down slope duration	1 s
Post-flow duration	30 s

operations have been characterised and compared to that of wrought Ti-6Al-4V. The chip morphology and the drill bit tool wear were also studied for the drilling trials. The findings obtained from this research work will contribute to a greater scientific understanding of the arc-wire-based additive manufacturing process and its influence on not only material properties but also machining characteristics.

2 Materials and methods

2.1 Materials

Commercially sourced Ti-6Al-4V plates with dimensions 250 mm × 100 mm × 12 mm were used as substrate material for the deposition trials. A Ti-6Al-4V wire 1 mm in diameter was used as filler wire for the gas tungsten arc welding (GTAW) additive manufacturing. The nominal chemical composition of the wire (in wt%) is provided in Table 1.

2.2 Gas tungsten arc welding

Welding was conducted using a water cooled Conley & Kleppen (CK) machine mount torch coupled to a Kemppi MasterTIG MLS 2000 inverter power supply with independent wire feed provided through a CK WF3 dedicated wire feed unit. The combined torch and wire feed arrangement was mounted above a linear actuator, with height adjustment possible through a manually operated rack-and-pinion. Inert gas shielding of the weld zone was achieved with welding grade pure argon using pre- and post-flow options. Additionally, a custom fabricated trailing shield was used to ensure that a sufficiently large shielding envelope was generated to the rear of the fusion zone to prevent post-weld atmospheric contamination of the successive weld beads. The general arrangement of GTAW equipment is illustrated in Fig. 1. Shielding gas flow rates and other common process parameters are detailed in Table 2.

Table 3 GTAW process parameters for preparation of additively manufactured Ti-6Al-4V samples for side milling trials

Sample ID	Arc energy (J/mm)	Specific deposition energy (kJ/g)	Passes	Total build height (mm)
Wall_02	482	21.0	35	29.0
Wall_03	525	16.2	27	28.8
Wall_04	504	12.1	21	29.0
Wall_05	497	12.1	24	29.9

2.3 Side milling

Side milling was carried out on the GTAW additively manufactured Ti-6Al-4V multi-layered deposited structures. A total of four build-up structures were produced using the process variables listed in Table 3. All structures consisted of a single weld pass per layer, producing a wall width of approximately 8 mm (schematic shown in Fig. 2a). For each sample an initial 'skimming' milling pass was performed to generate a smooth consistent surface such that the thickness of the wall was machined down to ~ 7 mm. The fabricated 'Wall_02' was used for an initial trial to validate the machining approach and the CNC G-code.[1] Moreover, to provide comparison to machining of wrought Ti-6Al-4V, a sample of similar geometry to the additively manufactured build-ups was fabricated from two sections of commercially sourced wrought Ti-6Al-4V plate measuring 200 mm × 50 mm × 12 mm. These were welded together in a T-fillet configuration (as shown in Fig. 2b) using 1 mm diameter Ti-6Al-4V filler wire. A 'double-V' preparation was used on the vertical plate to produce fully penetrated weld joint. Prior to the machining trials, the vertical wall section of this T-fillet was milled along its entire length, reducing its thickness to 7 mm to better match the geometry and rigidity of additive build-ups.

Milling trials were conducted in collaboration with Seco Tools Australia using a DMG MORI DMU 70 5-axis CNC milling machine. Samples were securely fastened to a Kistler 9257A three-component force dynamometer which was mounted to the milling machine table as shown in Fig. 3. The dynamometer was connected through three charge amplifiers to a computer where National Instruments (NI) LabVIEW was used to measure cutting forces in three directions. Side milling operations were performed on each sample

[1] The results from this test trial are not presented as this test was carried out for experimental setup and calibration.

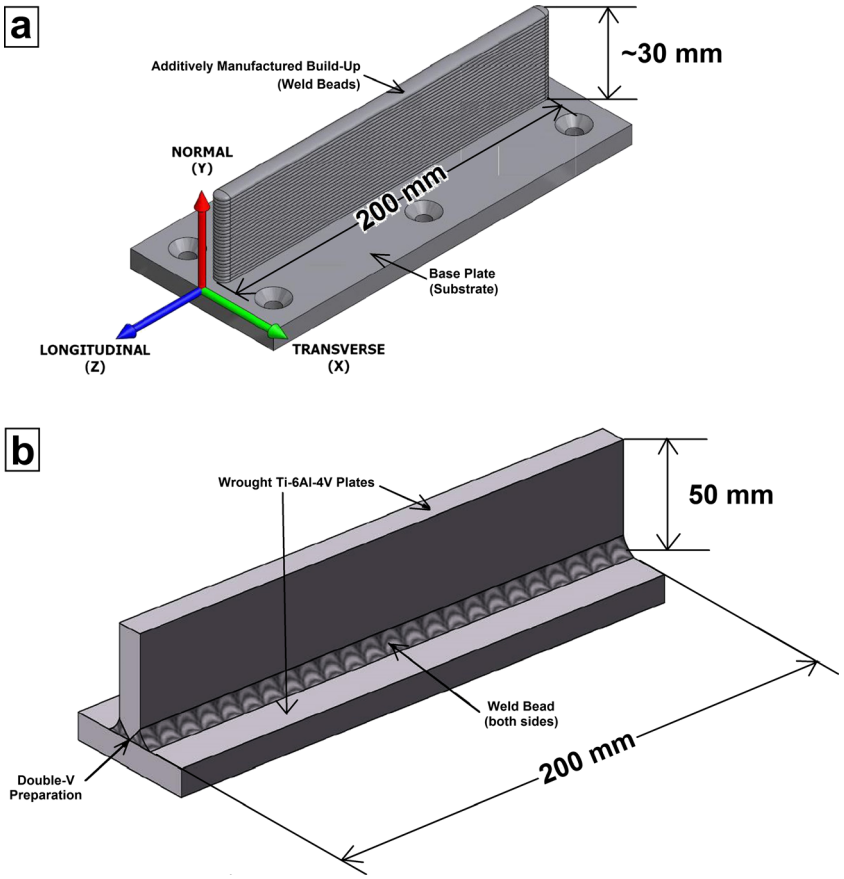

Fig. 2 Schematic illustration of **a** GTAW additively manufactured Ti-6Al-4V thin wall structure, and **b** T-fillet structure produced from wrought Ti-6Al-4V plates for side milling machining trials

using a 16-mm diameter SECO B39 JABRO HPM carbide end mill (designation JHP770160E2R250.0Z4A-SIRA) designed for machining of titanium alloys. The milling configuration, shown in Fig. 4, was selected to simulate the manufacture of deep pocketed, thin-walled features typical in structural aerospace components made from titanium alloys. A water-oil emulsion was applied as a coolant to the cutting zone at high pressure (60 bar) using directed nozzles and also through the spindle of the cutting tool. Other parameters relating to the machining process are given in Table 4.

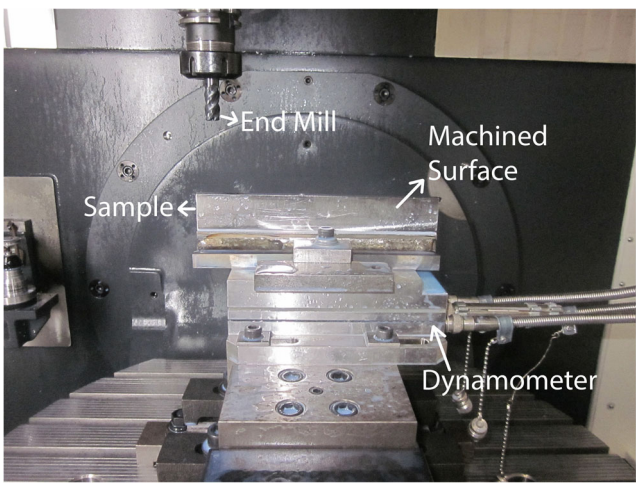

Fig. 3 General arrangement of equipment used for milling trials

The machinability of additively manufactured Ti-6Al-4V material produced by GTAW-wire based deposition was assessed relative to conventionally processed wrought material by comparing the machining forces during the side milling operation. The forces were considered in terms of those acting upon the cutting tool using a conventional Cartesian coordinate system as defined in Fig. 5. Using the measured forces in the radial (F_X) and feed (F_Z) directions, a single resultant force (F_R) acting on the cutting tool in the plane of the base plate was determined along with the angle of action (θ_R) relative to the feed direction.

Following the milling trials, surface finish was measured using a Hommelwerke T1000 profilometer and Turbo Datawin-NT 1.48 software. For each sample, the measurement range was 80 μm and the assessment length was set at 4.80 mm, running parallel to the feed direction. These surface profile measurements were converted to average surface roughness (R_a) values by the Turbo Datawin software according to ISO 11562.

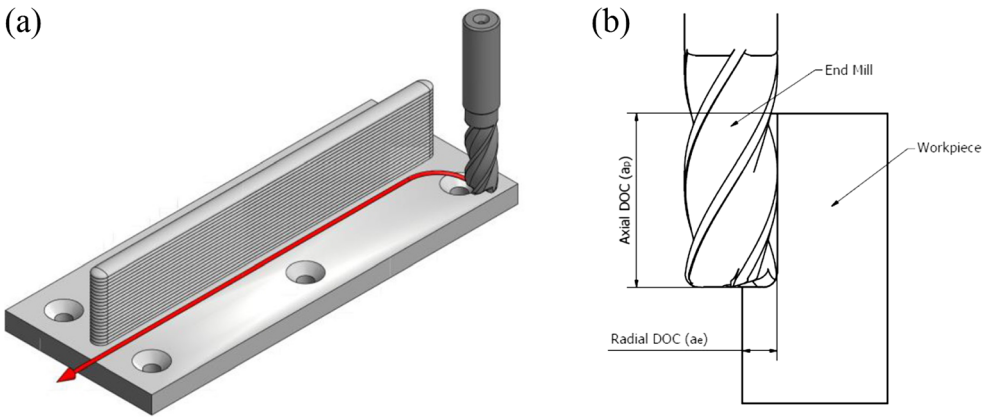

Fig. 4 Illustration of **a** tool path used and **b** depth of cuts (DOC) during the side milling trials

2.4 Drilling

A large pad-like deposit of Ti-6Al-4V was produced using the same welding equipment as described previously. A total of 100 weld beads were deposited in 11 layers using the parameters in Table 5, yielding a deposit approximately 250 mm in length, 40 mm in width and 20 mm in height as shown in Fig. 6. Despite the rigid clamping arrangement used during the welding process, the significant amount of thermal cycles experienced by the base plate during the deposition process caused a considerable amount of distortion in the base plate. As a result, the sample was prepared for drill testing by machining the bottom and top faces of the base plate (Fig. 6b) and the top of the deposit (Fig. 6c) to produce smooth flat surfaces for final clamping and drilling. An equivalent sample of wrought Ti-6Al-4V measuring 250 mm × 36 mm × 24 mm was cut from a large billet section 55 mm in thickness and machined flat on the top and bottom faces in preparation for drill testing.

Drilling trials were conducted in collaboration with Sutton Tools using a Haas TM-2P 3-axis CNC vertical milling machine, with samples securely fastened to a Kistler three-component force dynamometer which was mounted on the table of the milling machine. Again, the dynamometer was connected through three charge amplifiers to a computer where NI LabVIEW was used to measure cutting forces in three directions. Drilling operations were performed using 5 mm diameter (D) Sutton Tools R40 UNI stub drills, with a separate new drill used on each sample. Coolant (water-oil emulsion) was applied at standard pressure to the drill using directed nozzles. A total of 112 holes were drilled to a depth of 12.5 mm (2.5D) in each sample with holes arranged in a grid pattern of 4-by-28 holes at 8 mm centre spacing. While it is common practice in drill testing for holes to be randomly located within a material test piece to account for sample variability, the relatively uniform nature of the current samples as well as restrictions due to their size meant that the grid arrangement described above was adopted. Other parameters relating to the drilling process are given in Table 6. Cutting forces in all three directions were recorded for every

Table 4 Process parameters for side milling operations of the GTAW fabricated and wrought Ti-6Al-4V

Milling configurations	Climb (down) milling
Cutter diameter, D	16 mm
No. of teeth, z	4
Feed per tooth, f_z	0.15 mm/tooth
Feed per revolution	0.60 mm/rev
Surface cutting speed, V_c	80 m/min
Axial depth of cut, a_p	30 mm
Radial depth of cut, a_r	1 mm
Cutting length	~ 200 mm

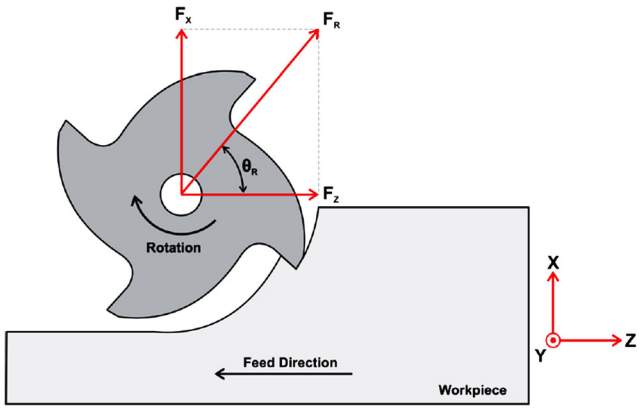

Fig. 5 Schematic representation of machining forces acting on the end mill cutting tool during side milling (F_x = Radial cutting force, F_y = Axial cutting force, F_z = Feed cutting force, F_R = Resultant cutting force in the X-Z plane)

Table 5 Summary of GTAW process parameters used to produce sample for drilling trials

Arc current	140 A
Arc length	4 mm
Travel speed	150 mm/min
Arc energy	634 J/mm
Wire feed speed	1470 mm/min
Specific deposition energy	18.9 kJ/g

Table 6 Process parameters for drilling operations used to assess machinability of GTAW fabricated Ti-6Al-4V

Drill diameter, D	5 mm
No. of flutes	2
Flute length, L_2	26 mm
Feed per revolution, f	0.09 mm/rev
Feed rate, V_f	51.5 mm/min
Surface cutting speed, V_c	9 m/min
Drill rotation	571 rev/min
Hole depth	12.5 mm
Hole count	112

fourteenth hole and compared to assess tool life and the relative machinability of the samples.

3 Results and discussion

3.1 Side milling of GTAW-fabricated Ti-6Al-4V

The cutting forces measured in the radial (F_X), axial (F_Y) and feed (F_Z) directions during the milling trials are shown in Fig. 7. In the case of F_X and F_Z, a similar profile is observed with the magnitude of forces increasing to a maximum value whereas F_Y decreases to a minimum value until the tool becomes fully engaged with the workpiece. The forces then oscillate about a steady-state value for the remainder of the machining process.

The initial peak in cutting forces is due to the tool path used, where the initial tool entry was through a circular arc originating at right angles to the wall and the tool exit path was parallel to the wall as illustrated in Fig. 4a. To achieve sequential full depth cuts, this tool path was offset by the required amount only in the radial (X) direction. It follows then that the maximum tool engagement is during the final section of the entry arc on the trailing side of the cutting tool. At this point, the radial depth of cut is equal to the full distance from the periphery of the tool to the outermost surface of the wall,

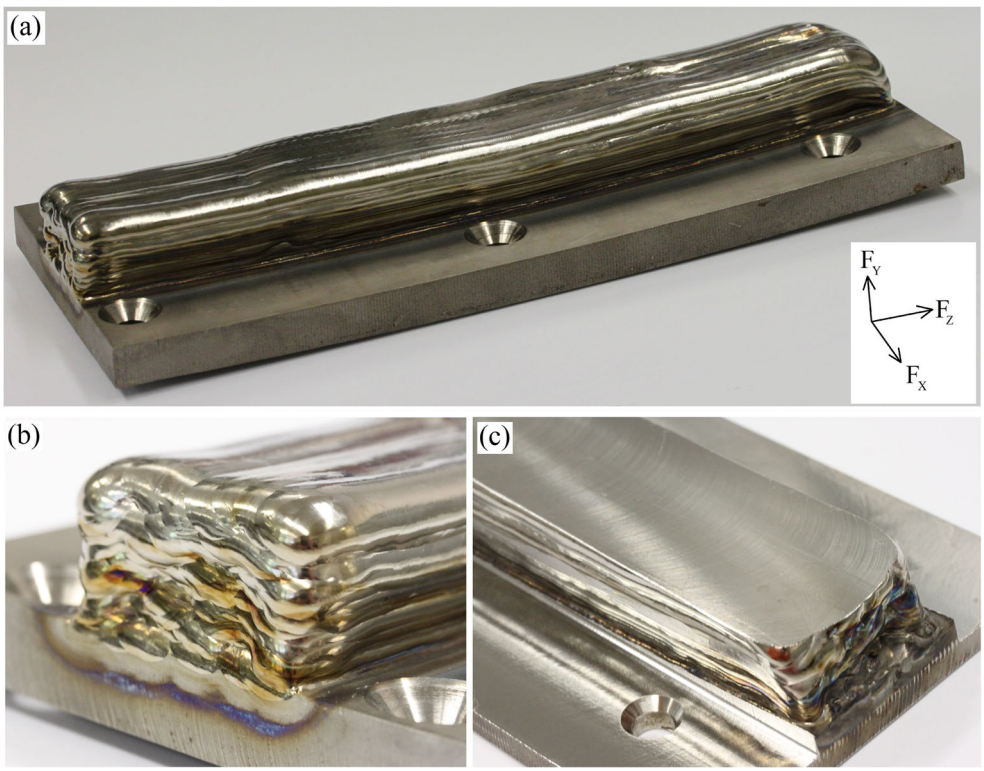

Fig. 6 **a** Additively manufactured pad sample for drill trials and **b** as-deposited, **c** machined flat in preparation for drill testing

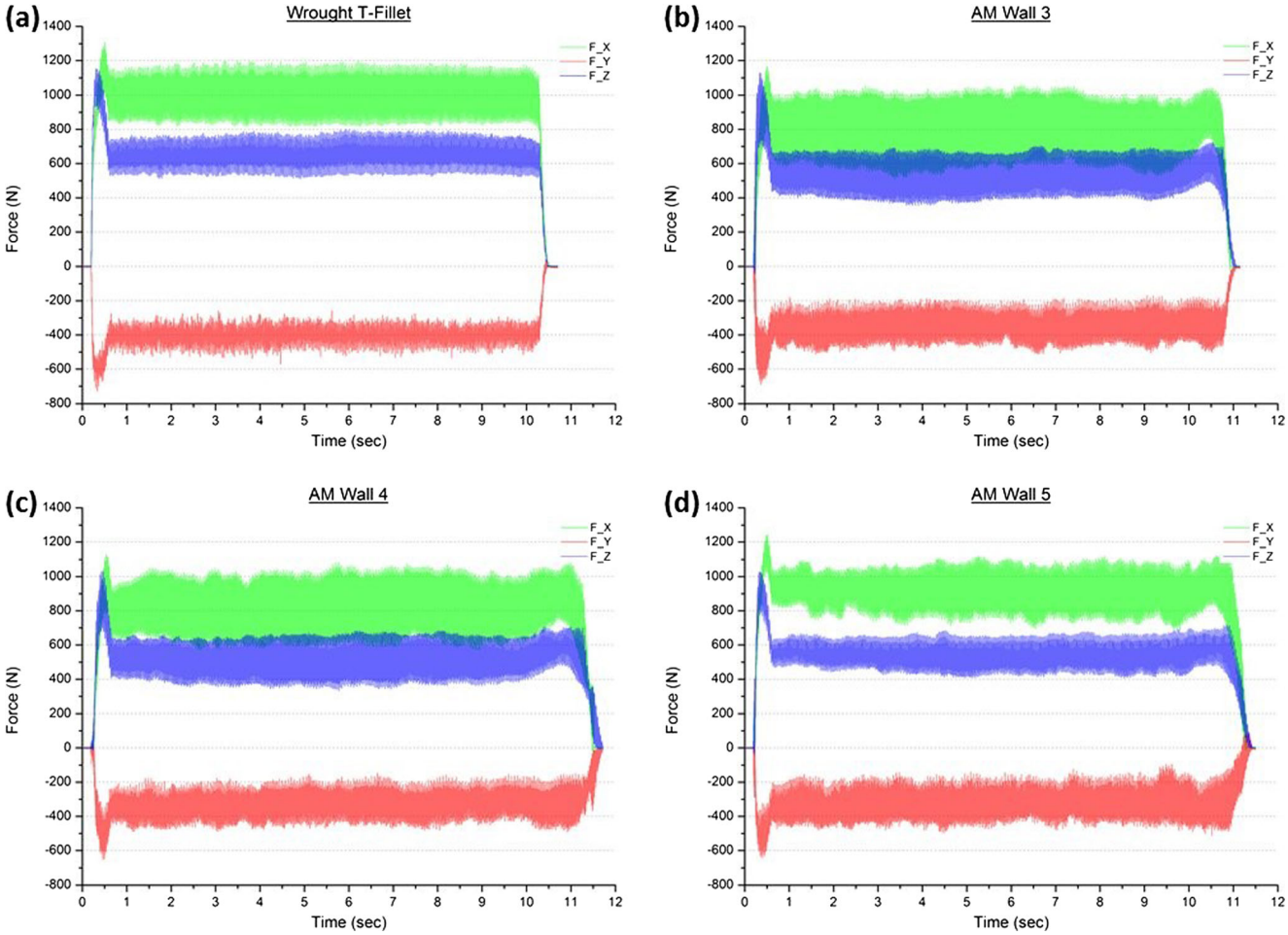

Fig. 7 Cutting forces in the radial (F_X), axial (F_Y) and feed (F_Z) directions presented as a function of time for **a** wrought T-fillet and **b**–**d** additively manufactured Ti-6Al-4V samples

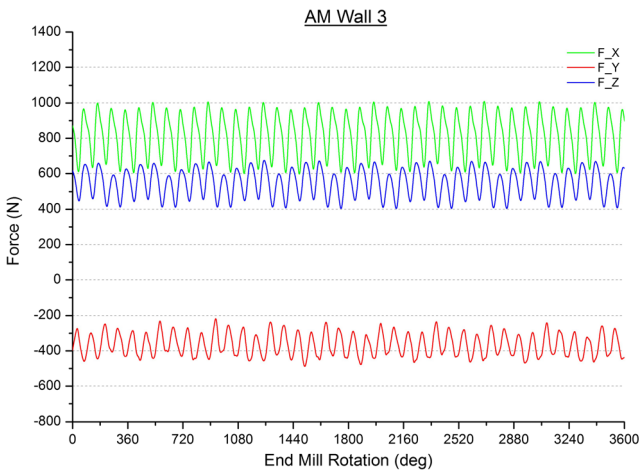

Fig. 8 Cutting forces in the radial (F_X), axial (F_Y) and feed (F_Z) directions as a function of tool rotation for milling of additively manufactured 'Wall_03'

producing the initial peak in cutting forces observed. López de Lacalle et al. [27] also reported the initial peak in the cutting forces due to the tool engagement during an end milling process.

The oscillations in the cutting forces are more clearly illustrated in Fig. 8 where the forces are plotted as a function of tool rotation angle. It can be observed that the primary source for the oscillation in cutting forces is the interrupted cutting characteristic of the milling process where engagement of individual cutting edges varies with tool rotation. This is a well-established understanding in milling dynamics [28]. Close observation of these oscillations reveals a periodic ramp-like increase of cutting forces repeated every four peaks. Since the end mill used in this study contained four cutting edges, each peak in cutting force corresponds to the maximum engagement of one single cutting edge. It is clear then that the periodic increase in cutting force is an indication of eccentricity in the cutting tool, resulting in non-uniform engagement of the four cutting edges [29].

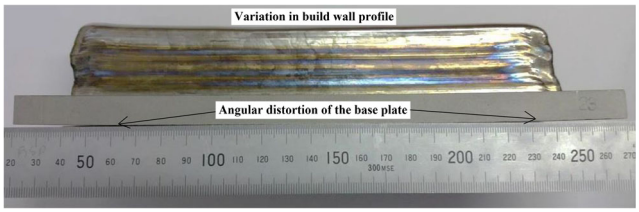

Fig. 9 Variation in build wall profile and the angular distortion of the base plate

Table 7 Average cutting forces during side milling of wrought and additively manufactured Ti-6Al-4V

Sample	Measured forces			Resultant	
	F_X (N)	F_Y (N)	F_Z (N)	F_R (N)	θ_R (deg)
Wrought T-fillet	966	− 406	642	1160	56.3
Additive Wall_03	815	− 354	546	982	56.1
Additive Wall_04	837	− 336	522	988	58.0
Additive Wall_05	912	− 337	545	1063	59.1

It can also be observed from Fig. 7 that the fluctuations in mean force values are more uniform for the wrought T-fillet sample whereas the additively manufactured samples displayed variation along the length of the machining pass. This suggests that the machining behaviour of the additively manufactured samples is not uniform along the length of the sample. The most likely causes for such inhomogeneity are thought to be the non-uniform wall profile in the as-deposited condition resulting in variable thickness along the length of the wall as well as slight angular distortion of about 5–7° at either ends of the base plate as shown in Fig. 9. This has also been reported by Ding et al. [30]. Moreover, another study reports that the surface inclination angle and tool's overhang has a significant influence on the generated forces and vibration during ball end milling operation [31].

From the plots in Fig. 7, it can be seen that the range of the high-frequency oscillations (seen as peak-to-peak 'fuzz' in the graphs) tends to be greater in samples of additively manufactured Ti-6Al-4V suggesting a greater variation in cutting edge engagement during the machining process. The most likely origin of this variation is wall deflection during machining. It should be noted that the height of the wall was different for the wrought samples (50 mm) as compared to the additively manufactured samples (30 mm). Even though the height engaged by the tool (30 mm) was the same for both wrought and additively manufactured workpieces, the difference in the total height of the samples may have resulted in different flexural stiffness [28]. Such oscillations can result in poor surface finish on the machined workpiece. This was verified by the surface profile measurements presented in Fig. 10. The corresponding average roughness (R_a) values for the wrought T-fillet and additively manufactured samples were 0.7 μm and 0.9 μm, respectively.

The average cutting forces measured during the side milling of additively manufactured and wrought Ti-6Al-4V samples is presented in Table 7. It was observed that the axial force (F_Y) was negative for all milling trials implying that the force on the cutting tool was downward toward the workpiece. This is expected as the end mill used in this study has a helix angle which provides an upward cutting action during milling [32].

From the data presented in Table 7, it can be seen that the radial force acting on the cutting tool is approximately 13% lower for additively manufactured samples during milling. A similar observation can be made in terms of cutting force in the feed direction where additively manufactured samples show 19% lower forces. Combining the feed and radial components into a single resultant force acting in the plane of the base plate, it is seen that in general, additively manufactured

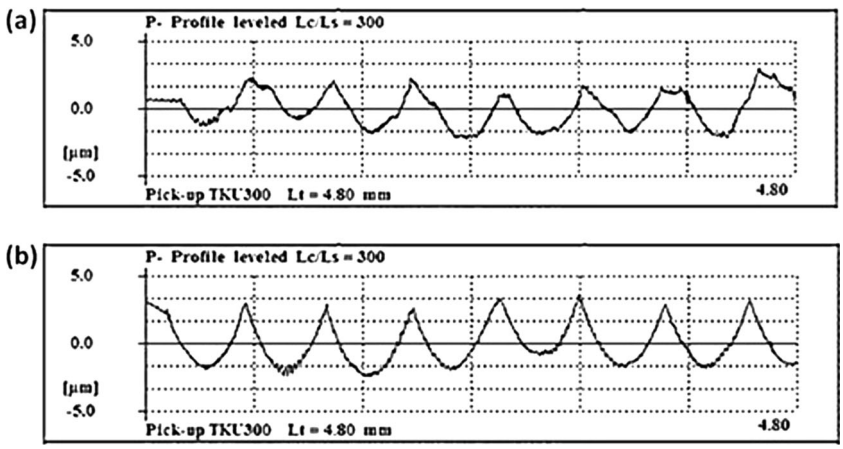

Fig. 10 Surface profile measurements of the machined surface in **a** wrought T-fillet and **b** additively manufactured Ti-6Al-4V samples

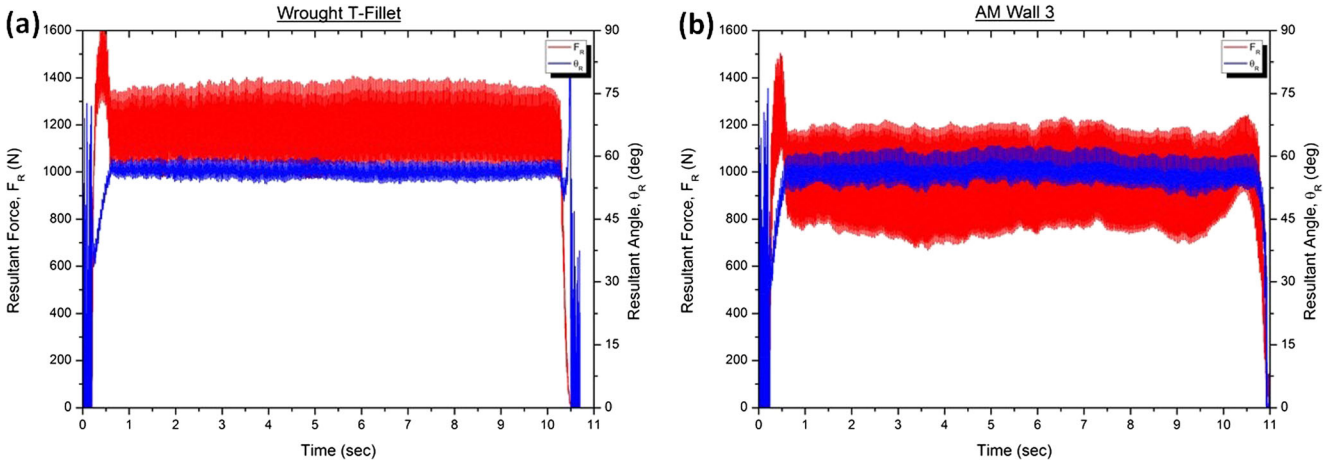

Fig. 11 Resultant cutting force magnitude and angle of action in the plane of the base plate for **a** wrought T-fillet and **b** GTAW-wire additively manufactured samples

samples required less cutting force than the wrought T-fillet sample during the machining operations. This is best illustrated in Fig. 11 which clearly shows a reduced magnitude of resultant force in additively manufactured Ti-6Al-4V with the angle of action approximately equal. It is also apparent that the axial force is considerably lower for machining samples of additively manufactured Ti-6Al-4V with a difference of between 17 and 21%. This can be directly correlated to the reduced hardness of the GTAW-AM wall as compared to the wrought plates used in fabricating the T-fillet section. The hardness of the AM coupons was lower by at least 20 HV (~ 6%) across all three planes as illustrated in Fig. 12.

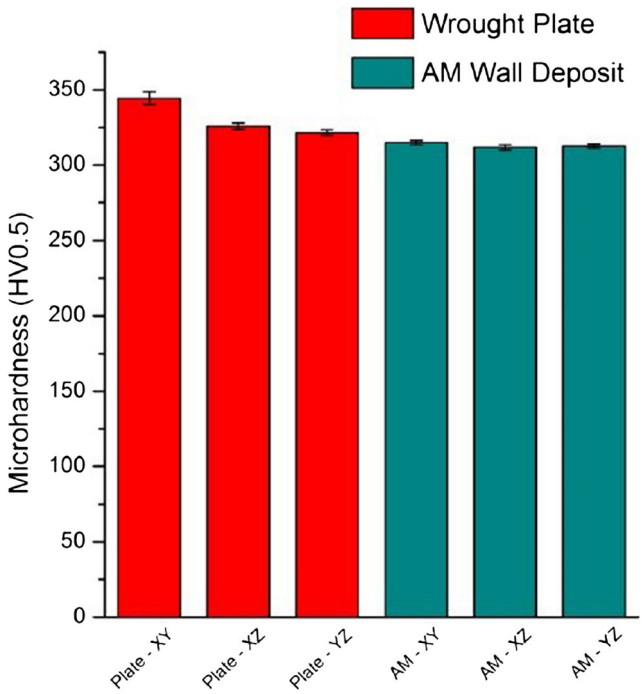

Fig. 12 Microhardness values for plate and additively manufactured Ti-6Al-4V

3.2 Drilling of GTAW-fabricated Ti-6Al-4V

Initial qualitative assessment of drill performance showed little difference between samples of wrought and additively manufactured Ti-6Al-4V with no change in acoustic emission or premature tool failures. In general, force measurements during drilling were as would be expected with force in the normal (Y) direction increasing to a steady state value while force in the transverse (X) and longitudinal (Z) directions oscillated about zero as shown in Fig. 13a [33]. Moreover, it was observed that the normal drilling force was higher by about 10–15% when drilling additively manufactured Ti-6Al-4V as shown in Fig. 13b. However, the transverse and the longitudinal drilling forces oscillated about zero, similar to the forces experienced by the tool when drilling wrought Ti-6Al-4V. The periodic nature of these oscillations corresponds to the rotation of the cutting edges on the drill, shown more clearly in Fig. 14.

Considering the profile of the normal force during the drilling operation, there appears to be five distinct zones as defined in Fig. 15. Zone I sees a sharp increase in force with little 'noise' in measured force data and corresponds to the initial contact between the drill tip and the workpiece. This is followed by Zone II where force continues to increase but at a lesser rate and with more noise in the measurements. This stage corresponds to the progressive engagement of the drill cutting edges, which produce the oscillations in measured force as shown in Fig. 14. Zone III sees a short period of approximately constant force which begins once the cutting edges of the

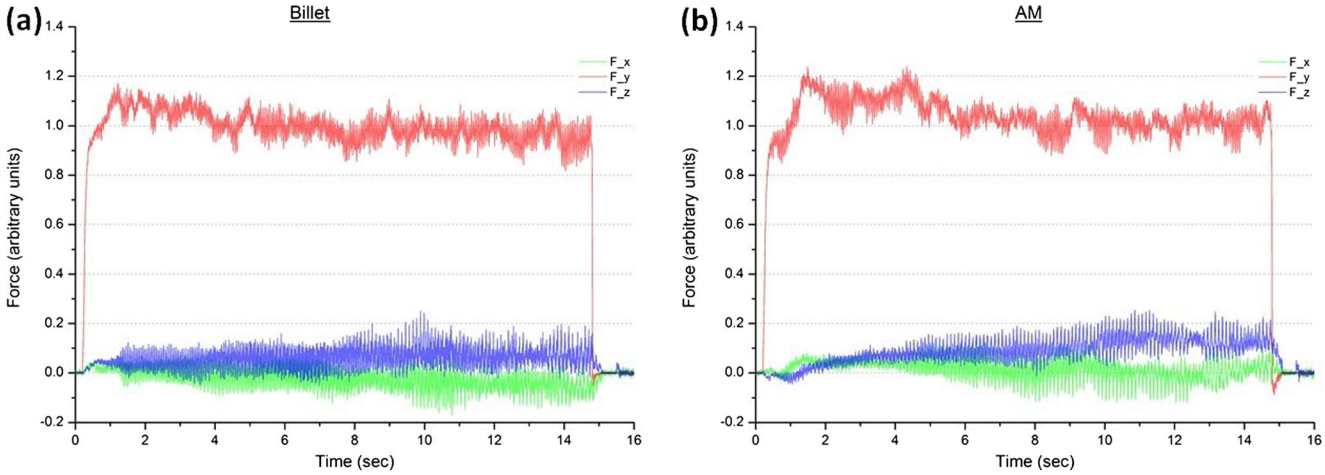

Fig. 13 Measured force values during drilling operations in samples of **a** wrought billet and **b** additively manufactured Ti-6Al-4V

drill are fully engaged, i.e. the hole is at full diameter. Normal force is then seen to drop slightly to a lower steady-state value for the remainder of the drilling operation, identified as Zone IV. Finally, Zone V sees a rapid drop in force as the drilling operation has achieved full depth and the drill is retracted from the hole. During this retraction, the normal force becomes slightly negative as the swarf laden drill tip is pulled from the top of the hole.

It should be noted that Zone III was more distinct in force data from the additively manufactured sample, whereas the transition between Zones III and IV was indistinguishable for several holes drilled in the wrought billet sample. For a homogeneous metal, it is thought that Zone III should not exist and force should reach and maintain a steady-state value from the time when full engagement of the cutting edges is achieved. For the case

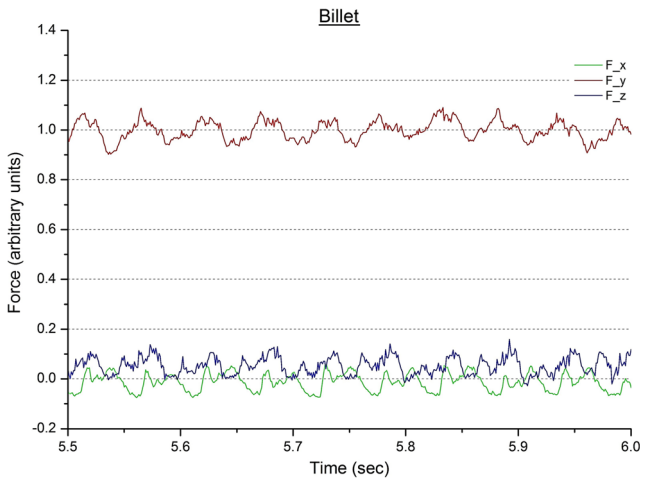

Fig. 14 Oscillations in measured force values during drilling of wrought billet

of the additively manufactured sample, the higher force in Zone III is thought to originate from the variation in the hardness with respect to the height of the additively manufactured Ti-6Al-4V pad. That is, several layers at the top of the pad had experienced fewer thermal cycles during deposition than the material in the preceding layers, thereby exhibiting higher hardness. The average hardness of the Ti-6Al-4V pad produced by GTAW-wire based additive manufacture (~ 325 HV) was about 8% higher than that of the wrought billet (~ 300 HV), clearly shown in Fig. 16.

Considering the variation in force as a function of the number of holes drilled, shown in Fig. 17, it is evident that forces in both the transverse and longitudinal directions are scattered about zero and no clear trend could be observed. In contrast, it is apparent that at all times, the drilling of additively manufactured Ti-6Al-4V required between 10 and 15% additional force in the normal direction to maintain the constant feed rate of 0.09 mm/rev. It is considered that the primary reason for this increased force is the higher hardness of the additively manufactured material when compared with the wrought sample.

It is also worth noting that the hardness values for this additively manufactured pad are greater than those of the additively manufactured wall features. The origin of these differences is most likely the different process parameters used as well as the differing arrangements of the sequential layers and the increased residual stress in the GTAW-AM Ti-6Al-4V pad resulting from the increased thermal cycling and deposition of greater volume of material as reported by Hoye et al. [34, 35]. On the other hand, the hardness of the billet used in the drilling trials is less than that of the wrought plates used for the side milling trials. This is due to the wrought plates being subjected to far greater amounts of thermomechanical deformation

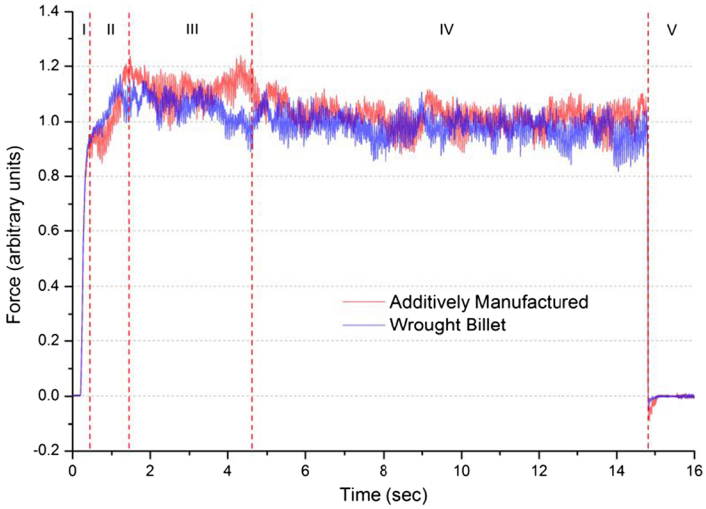

Fig. 15 Defined zones with respect to drilling force in the normal direction during drilling of both the wrought billet and the additively manufactured Ti-6Al-4V

operations against the fewer number of fabrication stages of the Ti-6Al-4V billet.

Qualitative examination of the swarf produced during drilling shows a typical 'curled ribbon' morphology for both the wrought and additively manufactured workpieces, with shorter, more broken segments produced from accumulation and compaction in the drill flutes where swarf ejection was compromised. Closer inspection revealed rougher surface finish in swarf from drilling of the wrought billet, with a more pronounced 'saw-tooth' type profile of burrs evident at the periphery, as seen in the higher magnification images presented in Fig. 18. This figure appears to show fracturing in some ribbon sections. Such breaks in the swarf could just as easily occur during ejection should there be an obstruction or restriction of some form in the flutes. This was the primary cause of considerably higher tool wear on the tip of the drill bits (as shown in Fig. 19) noticed after drilling 112 holes in wrought sample when compared to the drill bit used to machine GTAW-fabricated Ti-6Al-4V specimen. While neither drill showed significant loss of profile in the cutting edges, both did appear to show wear on the chisel point and a loss of the tool coating (TiAlN) in areas of the cone immediately behind the cutting edges. This loss of coating increased toward the periphery of the drill where cutting speeds were higher. From Fig. 19, it is apparent that there was a greater amount of wear on the margin of the drill used for the wrought

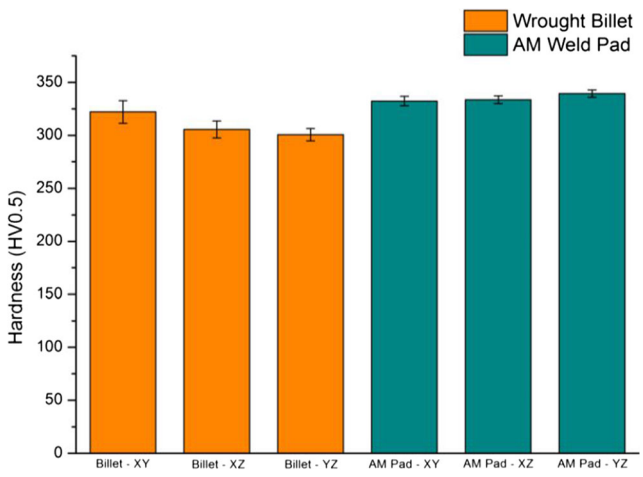

Fig. 16 Average microhardness of both wrought billet and additively manufactured samples as measured in three planes

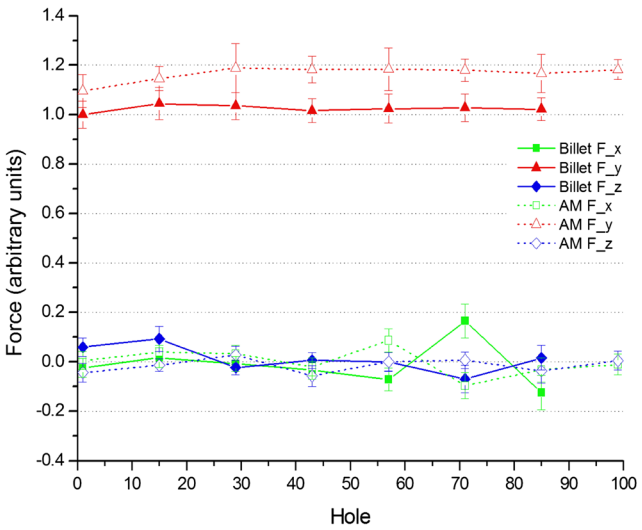

Fig. 17 Average forces during drilling as a function of number of holes drilled for both wrought billet and additively manufactured Ti-6Al-4V samples

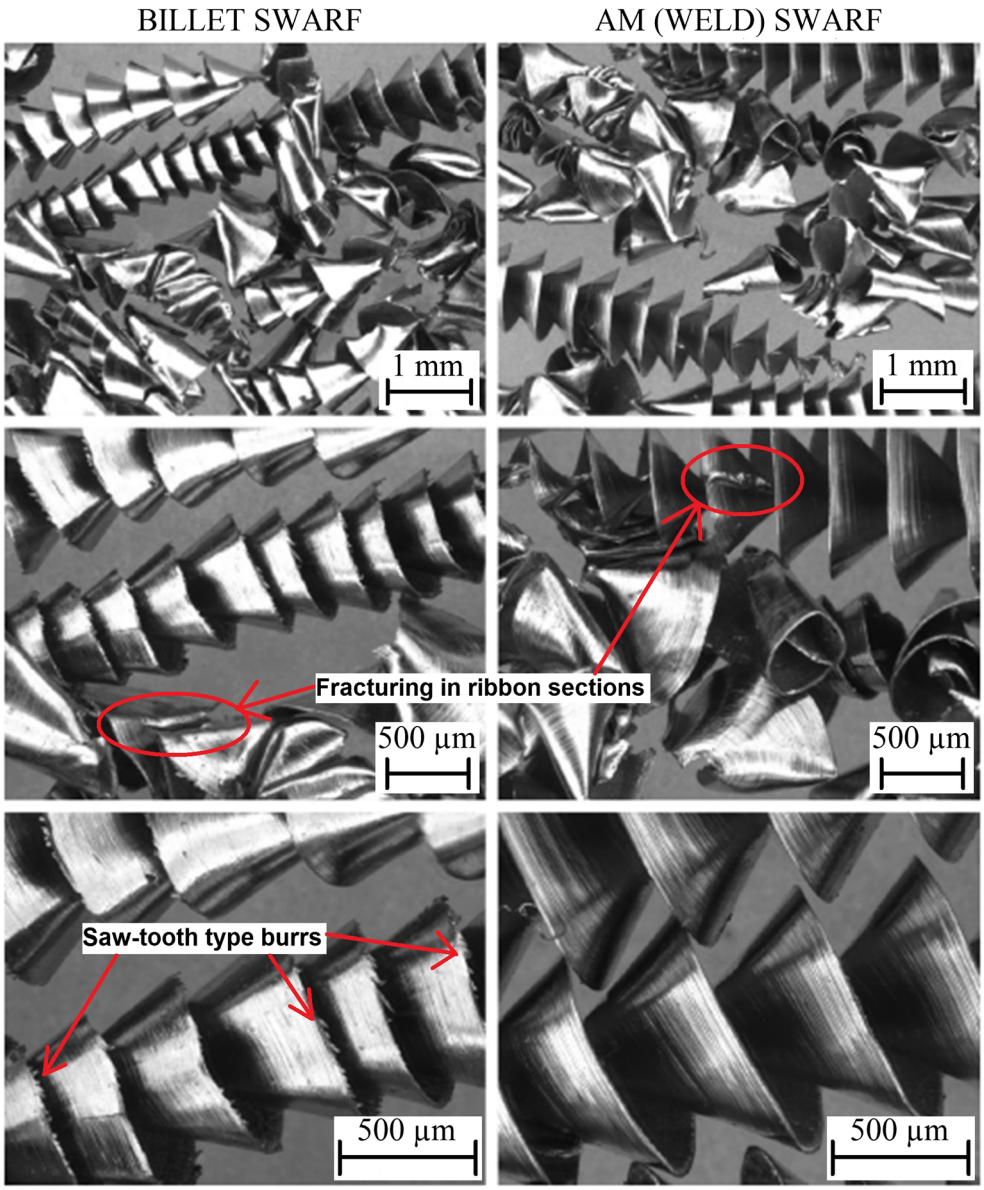

Fig. 18 Macroimages of swarf collected from drilling of left: wrought billet and right: additively manufactured Ti-6Al-4V

billet, with signs of tool chipping and build-up of the work-piece material which is usual when machining titanium alloys [24]. While such wear was not observed on the drill used in the additively manufactured sample, there is still evidence of built-up titanium on the margin toward the drill point. This is due to the marginally higher hardness of the additively manufactured pad which results in better material removal as opposed to the softer wrought billet [22].

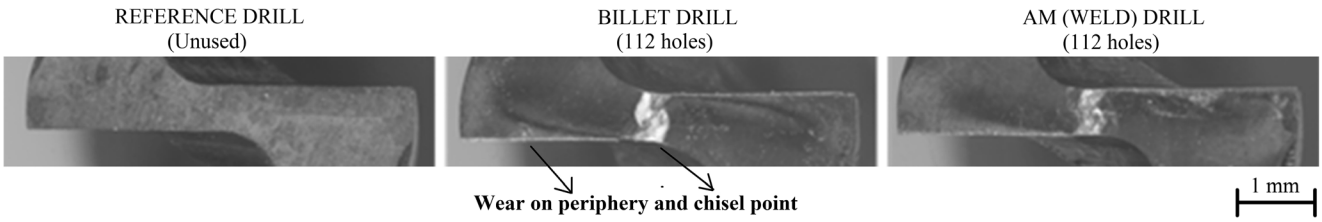

Fig. 19 Tool wear on the drill bits used to machine holes in the wrought and GTAW-fabricated Ti-6Al-4V

4 Conclusions

Machinability of the additively manufactured Ti-6Al-4V materials was investigated in terms of cutting forces generated during the milling and drilling trials. From the milling trials, it was found that the Ti-6Al-4V thin wall structures produced by GTAW additive manufacturing required lower cutting forces (by about 13–21%) in the three principal directions (radial (X), axial (Y) and feed (Z)) compared to an equivalent wrought structure which could be attributed to the lower hardness of the additively manufactured coupons. However, the oscillations of the cutting forces recorded for the GTAW-fabricated samples were larger resulting in high roughness ($Ra = 0.9$ μm) of the machined surface as compared to its wrought counterpart ($Ra = 0.7$ μm) due to the non-uniform wall thickness and the angular distortion of the base plate.

Conversely, the cutting forces were higher (by about 10–15%) when drilling the GTAW-fabricated pads compared to wrought titanium billet. In this case, it was found that the average hardness of the additively manufactured pad was about 8% higher than the wrought billet which contributed to the higher drilling force. However, the drill bits used for the wrought samples showed significantly more wear on the tool chisel tip than the drill bits used for the additively manufactured Ti-6Al-4V pad.

Overall, from this study, it can be concluded that the machinability of the Ti-6Al-4V produced by GTAW-wire-based additive manufacturing is better than the conventionally manufactured wrought titanium. Concerns regarding the machinability of GTAW-AM Ti-6Al-4V components are not justified and should not be seen as a barrier to future development and commercial implementation of this process.

Acknowledgements The authors gratefully acknowledge the support of Defence Materials Technology Centre (DMTC) for carrying out this work. The authors also acknowledge the assistance provided by Seco Tools for the milling trials and Sutton Tools for the drilling trials, results from which are presented in this manuscript.

References

1. Ezugwu EO, Wang ZM (1997) Titanium alloys and their machinability—a review. J Mater Process Technol 68:262–274
2. J.K. Wessel (2004) The handbook of advanced materials: enabling new designs, John Wiley & Sons
3. Rahman Rashid R, Bermingham M, Sun S, Wang G, Dargusch M (2013) The response of the high strength Ti–10V–2Fe–3Al beta titanium alloy to laser assisted cutting. Precis Eng 37:461–472
4. Bermingham MJ, Kent D, Zhan H, StJohn DH, Dargusch MS (2015) Controlling the microstructure and properties of wire arc additive manufactured Ti–6Al–4V with trace boron additions. Acta Mater 91:289–303
5. Bermingham MJ, Palanisamy S, Morr D, Andrews R, Dargusch MS (2014) Advantages of milling and drilling Ti-6Al-4V components with high-pressure coolant. Int J Adv Manuf Technol 72:77–88
6. Attar H, Ehtemam-Haghighi S, Kent D, Dargusch MS (2018) Recent developments and opportunities in additive manufacturing of titanium-based matrix composites: a review. Int J Mach Tools Manuf 133:85–102
7. P. Markillie (2012) A third industrial revolution: special report manufacturing and innovation, Economist Newspaper
8. Herzog D, Seyda V, Wycisk E, Emmelmann C (2016) Additive manufacturing of metals. Acta Mater 117:371–392
9. Qiu C, Ravi GA, Dance C, Ranson A, Dilworth S, Attallah MM (2015) Fabrication of large Ti–6Al–4V structures by direct laser deposition. J Alloys Compd 629:351–361
10. Vilaro T, Colin C, Bartout JD (2011) As-fabricated and heat-treated microstructures of the Ti-6Al-4V alloy processed by selective laser melting. Metall Mater Trans A 42:3190–3199
11. Bermingham MJ, Thomson-Larkins J, John DHS, Dargusch MS (2018) Sensitivity of Ti-6Al-4V components to oxidation during out of chamber wire + arc additive manufacturing. J Mater Process Technol 258:29–37
12. Murr LE, Quinones SA, Gaytan SM, Lopez MI, Rodela A, Martinez EY, Hernandez DH, Martinez E, Medina F, Wicker RB (2009) Microstructure and mechanical behavior of Ti–6Al–4V produced by rapid-layer manufacturing, for biomedical applications. J Mech Behav Biomed Mater 2:20–32
13. Ma Y, Cuiuri D, Hoye N, Li H, Pan Z (2015) The effect of location on the microstructure and mechanical properties of titanium aluminides produced by additive layer manufacturing using in-situ alloying and gas tungsten arc welding. Mater Sci Eng A 631: 230–240
14. Brandl E, Baufeld B, Leyens C, Gault R (2010) Additive manufactured Ti-6Al-4V using welding wire: comparison of laser and arc beam deposition and evaluation with respect to aerospace material specifications. Phys Procedia 5:595–606
15. Escobar-Palafox G, Gault R, Ridgway K (2011) Robotic manufacturing by shaped metal deposition: state of the art. Ind Robot 38:622–628
16. Pan Z, Ding D, Wu B, Cuiuri D, Li H, Norrish J (2018) Arc welding processes for additive manufacturing: a review, in. Springer Singapore, Singapore, pp 3–24
17. Short AB (2009) Gas tungsten arc welding of α + β titanium alloys: a review. Mater Sci Technol 25:309–324
18. Ben V, Jean-Pierre K (2007) Selective laser melting of biocompatible metals for rapid manufacturing of medical parts. Rapid Prototyp J 13:196–203
19. Luca F, Emanuele M, Pierfrancesco R, Alberto M, Simon H, Konrad W (2010) Ductility of a Ti-6Al-4V alloy produced by selective laser melting of prealloyed powders. Rapid Prototyp J 16: 450–459
20. M.J. Donachie (2000) Titanium: a technical guide, ASM international
21. Williams SW, Martina F, Addison AC, Ding J, Pardal G, Colegrove P (2016) Wire + arc additive manufacturing. Mater Sci Technol 32: 641–647
22. Rahman Rashid R, Sun S, Wang G, Dargusch M (2011) Machinability of a near beta titanium alloy. Proc Inst Mech Eng B J Eng Manuf 225:2151–2162
23. Bermingham MJ, Schaffarzyk P, Palanisamy S, Dargusch MS (2014) Laser-assisted milling strategies with different cutting tool paths. Int J Adv Manuf Technol 74:1487–1494
24. Rahman Rashid RA, Palanisamy S, Sun S, Dargusch MS (2016) Tool wear mechanisms involved in crater formation on uncoated carbide tool when machining Ti6Al4V alloy. Int J Adv Manuf Technol 83:1457–1465

25. Bolar G, Das A, Joshi SN (2018) Measurement and analysis of cutting force and product surface quality during end-milling of thin-wall components. Measurement 121:190–204
26. Wojciechowski S, Maruda RW, Barrans S, Nieslony P, Krolczyk GM (2017) Optimisation of machining parameters during ball end milling of hardened steel with various surface inclinations. Measurement 111:18–28
27. López de Lacalle LN, Lamikiz A, Sánchez JA, Salgado MA (2007) Toolpath selection based on the minimum deflection cutting forces in the programming of complex surfaces milling. Int J Mach Tools Manuf 47:388–400
28. Cheng K (2009) Machining dynamics fundamentals. Applications and Practices, Springer, London
29. Armarego EJA, Deshpande NP (1991) Computerized end-milling force predictions with cutting models allowing for eccentricity and cutter deflections. CIRP Ann 40:25–29
30. Ding D, Pan Z, Cuiuri D, Li H (2015) Wire-feed additive manufacturing of metal components: technologies, developments and future interests. Int J Adv Manuf Technol 81: 465–481
31. Wojciechowski S, Maruda RW, Krolczyk GM, Niesłony P (2018) Application of signal to noise ratio and grey relational analysis to minimize forces and vibrations during precise ball end milling. Precis Eng 51:582–596
32. S. Palanisamy, R. Rashid, M. Brandt, S. Sun, M. Dargusch (2014) Comparison of endmill tool coating performance during machining of Ti6Al4V alloy. Adv Mat Res 974
33. Li R, Hegde P, Shih AJ (2007) High-throughput drilling of titanium alloys. Int J Mach Tools Manuf 47:63–74
34. Hoye N, Li HJ, Cuiuri D, Paradowska A (2014) Measurement of residual stresses in titanium aerospace components formed via additive manufacturing, in: 7th International Conference on Mechanical Stress Evaluation by Neutrons and Synchrotron Radiation, MECA SENS 2013. Sydney, NSW, pp 124–129
35. N. Hoye, H. Li, D. Cuiuri, A. Paradowska, K. Thorogood (2014) Investigation of residual stresses in titanium aerospace components formed via additive manufacturing. In: Das R, John S (eds) 8th Australasian Congress on Applied Mechanics, ACAM 2014, as Part of Engineers Australia Convention 2014, Engineers Australia, pp. 933–941